Contraction in Voltage-Clamped, Internally Perfused Single Heart Cells

BARRY LONDON and JOHN W. KRUEGER

From the Departments of Physiology/Biophysics and Medicine, Albert Einstein College of Medicine, Bronx, New York 10461

ABSTRACT We studied contraction in single voltage-clamped, internally perfused myocytes isolated from guinea pig ventricles. The microscopic appearance of the cell was observed and recorded with a television system, while contractile shortening was measured 1,000 times/s using a linear photodiode array. Uniform, synchronous sarcomere shortening occurred in response to depolarizations that triggered a slow inward current (I_{si}). Changes in I_{si} caused by altering the amplitude of the voltage step, the extracellular [Ca^{2+}], or the holding potential were accompanied by immediate parallel changes in the extent and velocity of shortening. In particular, twitch shortening during depolarization (*a*) was immediately decreased when large voltage steps decreased I_{si}, and (*b*) was eliminated by depolarizations that exceeded +75 mV, the apparent reversal potential for Ca^{2+}. In these cases, shortening was associated with the tail current during repolarization. Increases in the amplitude, duration, and the rate of the depolarizing step increased the extent and speed of sarcomere shortening over the course of four to five contractions without a simultaneous parallel increase of I_{si}. Large prolonged depolarizations caused an asynchronous, nonuniform, oscillatory shortening of the cell and potentiated future twitch contractions. Increases in the duration of the depolarizing step immediately prolonged contraction; otherwise, interventions that altered the extent, velocity, and time course of shortening in intact, nonperfused cells did not affect the time course of the contraction in the internally perfused single cells. Our results provide direct support for the hypothesis that I_{si} both induces and grades the size of the Ca^{2+} release from the sarcoplasmic reticulum of intact cardiac muscle. In addition, a separate, depolarization-dependent process unrelated to I_{si} (*a*) grades the size of contraction, presumably by modulating Ca^{2+} accumulation in the intracellular stores, and (*b*) affects its time course.

INTRODUCTION

The prevailing theory of excitation-contraction (E-C) coupling in mammalian cardiac muscle is that the transsarcolemmal Ca^{2+} influx during an action potential causes a large release of Ca^{2+} from the sarcoplasmic reticulum (SR) (Fabiato,

Address reprint requests to Barry London, Division of Cardiology, Dept. of Medicine and Physiology/Biophysics, Albert Einstein College of Medicine, Forchheimer Bldg., Rm. G54, 1300 Morris Park Ave., Bronx, NY 10461.

J. GEN. PHYSIOL. © The Rockefeller University Press · 0022-1295/86/10/475/31 $1.00

Volume 88 October 1986 475–505

1983; Chapman, 1983). This process is known as Ca^{2+}-induced Ca^{2+} release. The clearest evidence in support of Ca^{2+}-induced Ca^{2+} release comes from studies on single heart cells, where the sarcolemma is removed by mechanical dissection, leaving the internal membranes intact (Fabiato, 1981, 1983; Fabiato and Fabiato, 1975). Under these conditions, contractions are induced and graded in amplitude by increments in $[Ca^{2+}]$ that are insufficient to activate the myofilaments directly.

In cardiac muscle with fully intact membranes, however, the processes that determine the size and time course of the twitch contraction are less well defined (Chapman, 1983; Fozzard, 1977). The extent to which the inward current raises the intracellular $[Ca^{2+}]$ depends on the Ca^{2+}-buffering capacity of each cell. Voltage-clamp studies that sought to clarify the role of the inward Ca^{2+} current have described two types of contraction (phasic and tonic). These types are related in different ways to depolarization and to the inward current, and their microscopic features are not known. Moreover, the amount of Ca^{2+} stored in the SR probably plays a key role in determining contractility. Thus, it is difficult to define the exact role of the Ca^{2+}-induced Ca^{2+} release process in the intact cell.

The single, isolated cardiac muscle cell differs in several important respects from multicellular preparations. Its simple geometry and large electrical space constant permit rapid and uniform control of the membrane potential (Brown et al., 1981; Lee and Tsien, 1982). Internal perfusion through a suction electrode allows the composition of the cytoplasm to be modified. Ion accumulation in narrow intercellular spaces is eliminated. Moreover, the unattached intact cell constitutes a discrete and uniform population of sarcomeres that shorten synchronously in response to electrical stimuli (Krueger et al., 1980; Roos et al., 1982). As such, the single heart cell is an ideal preparation for the study of the cardiac E-C coupling process.

Several recent studies have examined shortening in single isolated cardiac myocytes using one- or two-microelectrode voltage clamps (Isenberg et al., 1985; Mitchell et al., 1984, 1985). Isenberg et al. concluded that depolarization alone (without I_{si}) may trigger a rapid release of Ca^{2+} from the SR, and that Ca^{2+} entering the cell via the slow inward current may directly activate another, slower component of contraction. Mitchell et al. (1985) concluded that Ca^{2+} stored in the SR plays a key role in the contraction of rat myocytes, but possibly a less important role in the contraction of guinea pig heart cells (Mitchell et al., 1984).

We have modified a whole-cell voltage-clamp technique to simultaneously measure contractile shortening and transmembrane current in internally perfused single heart cells. Thus, we can study cardiac E-C coupling under conditions that allow (*a*) good voltage control and accurate measurement of transmembrane current, (*b*) uniform activation and an accurate measure of contraction, and (*c*) direct access to the intracellular environment, available previously only in preparations without external membranes. This approach allows us to test directly some interpretations derived originally from separate experiments on either intact muscle or skinned cells. It also provides very specific insights into the mechanisms that govern contraction in cells with intact membrane systems.

Some of the results in this study have appeared previously in abstract form (London and Krueger, 1985).

METHODS

Preparation of Isolated Cardiac Muscle Cells

Ca^{2+}-tolerant single heart cells were isolated from the ventricles of 300–500-g adult male guinea pigs using the general technique established by Haworth et al. (1980). The animals were anesthetized with ether and killed by cervical dislocation. The heart was rapidly excised and the coronary vessels were retroperfused via the aorta with an oxygenated (95% O_2, 5% CO_2) physiological salt solution (composition [mM]: 118 NaCl, 4.8 KCl, 1.2 KH_2PO_4, 1.2 $MgSO_4$, 11 glucose, 25 $NaHCO_3$, 1.0 $CaCl_2$) at 37°C. When the blood was cleared away, 60 ml of the salt solution, with no added Ca^{2+}, was washed through the heart, and then 40 ml of the solution, with between 0.20 and 0.25 mg/ml collagenase (Worthington Biochemical Corp., Freehold, NJ) added, was recirculated through the heart for 15 min. The ventricles were then minced, and the tissue was shaken for 30-min periods in 10-ml aliquots of the same collagenase-containing solution with 1.0 mM $CaCl_2$ added. An additional 0.20 mg/ml of collagenase and 0.20 mg/ml of hyaluronidase (Sigma Chemical Co., St. Louis, MO) were usually added during the first 30-min period. After each period, single cells were separated from the remaining tissue and stored at room temperature in a HEPES-buffered, physiological salt solution (composition [mM]: 118 NaCl, 4.8 KCl, 1.2 KH_2PO_4, 1.2 $MgSO_4$, 11 glucose, 25 NaHEPES, 2.5 $CaCl_2$, pH 7.4).

Some cells were placed in a delrin chamber (total volume, 3 ml) filled with the HEPES-buffered physiological salt solution. The cells settled onto the microscope coverslip that made up the bottom of this chamber, and were viewed with an inverted microscope (Ernst Leitz GmbH, Wetzlar, Federal Republic of Germany) equipped with a 40×, 0.65-NA phase-contrast objective, a third tube, a direct current–powered illuminator, and a heat filter. All experimental solutions, excluding those used in the cell-isolation procedure, were filtered (0.22-μm filters, Millipore Corp., Bedford, MA) to remove particulate matter.

Contraction of Intact Cells

An extracellular microelectrode (tip diameter, 1 μm) was filled with the bath solution and placed near a cell's membrane. A second platinum electrode was dipped into the bath on the opposite side of the cell. Contraction was triggered by constant-current, 5-ms, negative-polarity pulses through the pipette.

Whole-Cell Voltage Clamp

Suction micropipettes, with tip diameters of 2–8 μm (0.5–2.0 MΩ resistance when filled), were pulled (model 700C, David Kopf Instruments, Tujunga, CA) from flint glass (3 mm o.d., Friedreich and Dimmock, Inc., Millville, NJ) and lightly fire-polished (Hamill et al., 1981). Each pipette was filled with intracellular perfusate (see below), mounted in a holder apparatus (Brown et al., 1981), and brought near the cell with a hydraulic micromanipulator (model MO-102, Narishige Scientific Instruments Laboratory, Tokyo, Japan). A high-resistance seal (>500 MΩ) was formed between the pipette and cell by gentle suction (Fig. 1). The cell membrane was broken by a large brief negative pressure, and the cell was then internally perfused and voltage-clamped (circuit designed and constructed by Dr. Lawrence Eisenberg, The Rockefeller University, New York). The resistance of each pipette was measured before the approach to the cell, and series resistance compensation (up to 1.5 MΩ) was used to negate this voltage drop across the pipette. The solution in the pipette could be rapidly changed via a solution line near its tip. 30 μM tetrodotoxin (TTX) was added to the extracellular solution to decrease the Na^+ current through the fast Na^+ channels.

Measurement of the Ca^{2+} Current

Depolarizing steps from a holding potential of −50 mV triggered the slow inward current (I_{si}). I_{si} is usually attributed to an intactivating inward Ca^{2+} current through highly selective voltage-dependent Ca^{2+} channels (Lee and Tsien, 1984; Matsuda and Noma, 1984). Fig. 2*A* shows the current-voltage relationship of one internally perfused cell at the peak of the inward current and at the steady state 300 ms after the clamp step.

We wished to use the difference between the peak inward current and the current at 300 ms ($I_{peak} - I_{300}$) as a measure of the peak inward Ca^{2+} flux. There are several potential

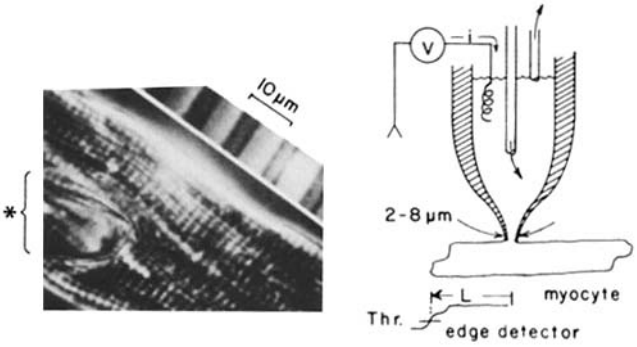

FIGURE 1. (*Left*) The appearance of an internally perfused voltage-clamped single heart cell, viewed with a 40× phase-contrast objective. The image of the cell was photographed from a television monitor. The asterisk denotes the tip of the suction pipette, which is pushing down on and flattening the center of the cell. The holding potential was −50 mV, and the cell was at rest and quiescent. This cell had a sarcomere length of 1.88 μm, which was uniform throughout. A 10-μm grating is shown in the upper right for scale. (*Right*) A schematic representation of this preparation. The voltage (V) inside the pipette is monitored, and current (i) is passed into the pipette to maintain the voltage at the desired level. The internal perfusate is delivered near the tip of the pipette by one solution line; another line removes excess solution and maintains suction within the pipette. The bottom trace represents the light intensity as recorded by the photodiode onto which an image of the cell is projected. The edge detector interprets all areas of the field where the light intensity exceeded threshold ("Thr.," horizontal line) as being part of the cell. The threshold was set manually for each experiment.

problems with this measurement, however (Lee and Tsien, 1984; Isenberg and Klockner, 1982). To the extent that the Ca^{2+} current does not fully inactivate in 300 ms (Lee and Tsien, 1982; Isenberg and Klockner, 1982; Gibbons and Fozzard, 1975), this measure will underestimate the true value of the inward Ca^{2+} flux. Moreover, other ions (through other channels) may contribute to the time-dependent currents measured under voltage clamp, especially given the complex nature of the internal and external solutions necessary to permit cell shortening (see below). These would include several of the time-dependent outward K^+ currents described in this preparation (Iijima et al., 1985; Matsuda and Noma, 1984; Isenberg and Klockner, 1982).

To evaluate these issues, the Ca^{2+} channels were blocked by the addition of 100 μM verapamil or 100 μM Cd^{2+} to the bath (Fig. 2). Several features were notable. (*a*) Verapamil (or Cd^{2+}) almost completely eliminated the time-dependent inward current (Fig. 2*A*).

Neither agent fully eliminated the negative slope conductance region of the *I-V* curve, which can be attributed in part to the inwardly rectifying K^+ channel (Kurachi, 1985; Noble, 1984). (*b*) The current-voltage curves suggest that the Ca^{2+} current was not fully inactivated 300 ms after the voltage step. (*c*) For large voltage steps, there was a slowly activating outward current (at these voltages, an inactivating inward current is unlikely), which was also seen (although to a lesser extent) in the presence of verapamil or Cd^{2+}. This current probably explains why $I_{peak} - I_{300}$ does not reach zero for large voltage steps (Figs. 2, *B* and *C*, and 8*C*), and was seen under the same conditions that cause steady shortening of the cell (see Fig. 5). (*d*) There was a small change in the holding current after the addition of the channel blockers. This could be explained by a change in the background K^+ conductance, which may have been a result of the drug or a change in the condition of the cell during the 15 min between the two measurements. In any case, the error in the values of the net current should be small at potentials above −30 mV because of the inward-going rectification of the K^+ channels.

A general concern arises from the possibility that an early outward time-dependent K^+ current may mask a part of I_{si}. Josephson et al. (1984*a*, *b*) did not find an early outward K^+ current in single guinea pig myocytes. They did find an early outward current in rat myocytes, but it was not Ca^{2+} dependent and it was completely inactivated at holding potentials of −50 mV. Mitra and Morad (1985) also failed to find a Ca^{2+}-dependent outward current in guinea pig and rabbit ventricular myocytes. Finally, the time dependence of the inwardly rectifying K^+ channel (I_{K1}) is sufficiently rapid that it should not interfere with measurements of I_{si} (Kurachi, 1985).

In addition, the verapamil/Cd^{2+}-sensitive current was determined by digitally subtracting the current 10 min after the addition of the channel blocker from the current before its addition. This estimate of the inward Ca^{2+} current compared favorably with $I_{peak} - I_{300}$ over a wide range of voltage steps (Fig. 2, *B* and *C*). There was a reversal of the verapamil/Cd^{2+}-sensitive Ca^{2+} current above +60 mV, however (Fig. 2, *B* and *C*; Lee and Tsien, 1982). The verapamil/Cd^{2+}-sensitive current exceeded $I_{peak} - I_{300}$ by <20% for voltage steps to 0 mV. This is further evidence that a Ca^{2+}-independent early outward current did not hide a significant part of the Ca^{2+} current at a holding potential of −50 mV.

The channel blockers eliminated the twitch shortening and therefore the Ca^{2+} transient; thus, the verapamil/Cd^{2+}-sensitive current included not only the inward Ca^{2+} current but also any Ca^{2+}-dependent currents that accompanied twitch contraction. Rapid oscillations in cytoplasmic Ca^{2+} triggered only very small currents at potentials above 0 mV, however (see Fig. 5); this suggests that, at these voltages, the Ca^{2+}-dependent currents are rather small.

In summary, these results confirm that $I_{peak} - I_{300}$ gives a good estimate of the magnitude of the peak current through the verapamil/Cd^{2+}-sensitive Ca^{2+} channel for voltage steps to ~0 mV. Above this potential, I_{si} decreases and eventually disappears.

Intracellular Perfusate

The internal perfusate was weakly buffered at pCa 7 with 0.5 mM EGTA (Fabiato, 1981; Fabiato and Fabiato, 1979). It contained (in mM): 89.4 K-aspartate, 7.1 $MgSO_4$, 5.0 glucose, 30.0 TES (*N*-tris[hydroxymethyl]methyl-2-aminoethane sulfonic acid, a pH buffer), 0.131 KCaEGTA, 0.369 K_2EGTA, 3.3 K_2ATP, 3.75 Na_2CP (creatine phosphate), 8.25 $Tris_2$CP, 0.03 NacAMP, 0.1 DTT (dithiothreitol, a reducing agent), and 30 U/ml CPK (creatine phosphokinase), and was brought to pH 7.1 with ~11 mM KOH. Cells were unstable with lower concentrations of EGTA in the internal perfusate. Twitch shortening in response to depolarizing stimuli occurred with EGTA concentrations as high as 0.8 mM. MgATP was essential for the occurrence of twitch shortening. After the

onset of internal perfusion, changing to a dialysate with no added MgATP caused rigor shortening after 15–30 s, which was followed by a rigor-like state. The cell relengthened upon reperfusion with 5 mM MgATP.

In preliminary experiments, 30.6 mM Na^+ was used in the intracellular perfusate. Under these conditions, contracture shortening developed in the vicinity of the pipette and slowly spread throughout the cell. This may have been due to Na/Ca exchange (Blaustein and Nelson, 1982; Sheu and Fozzard, 1982).

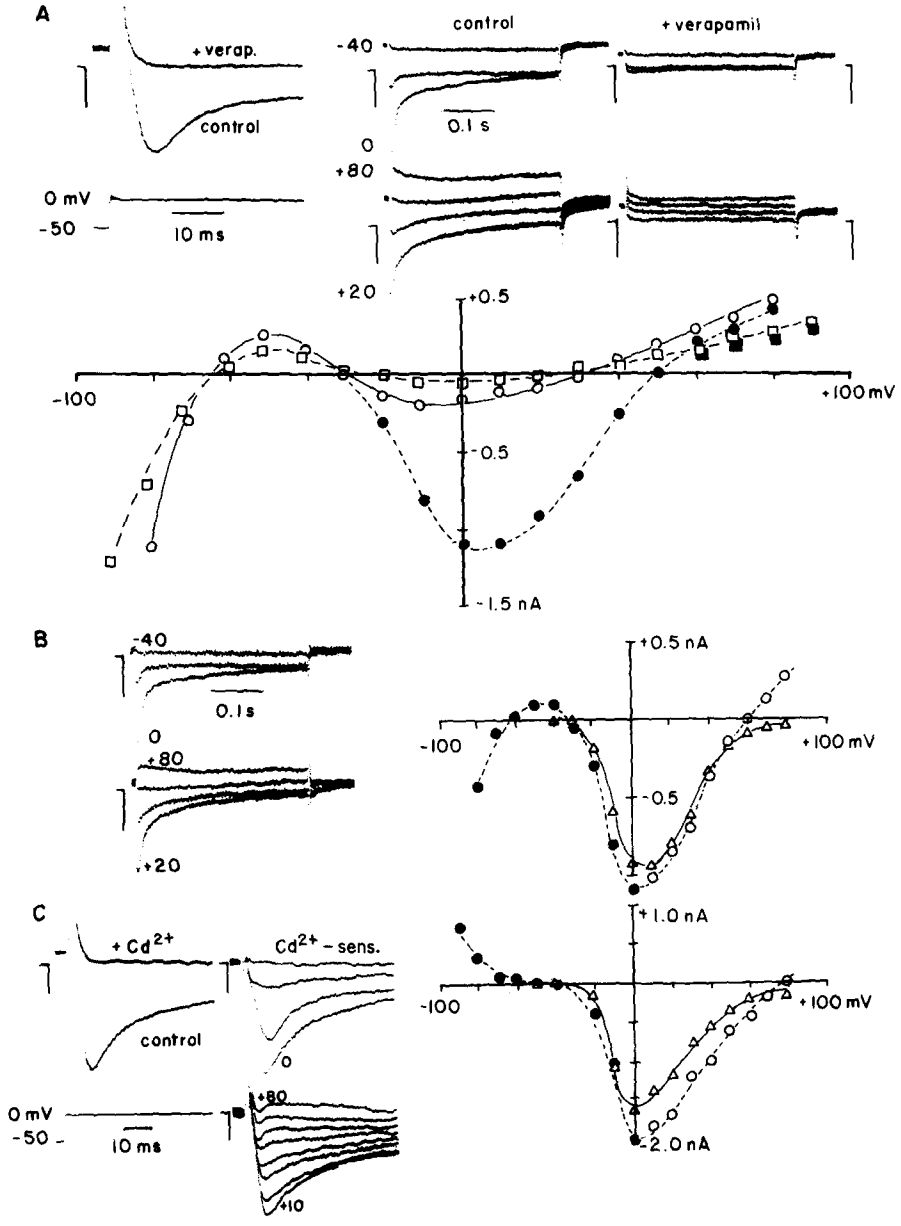

Cell and Sarcomere Length Measurement

Each cell selected for study was oriented with its long axis parallel to a self-scanned, linear photodiode array (model 256 C/17, EG&G Reticon, Sunnyvale, CA) and then approached by the suction electrode. A television system was used to monitor the cell and the pipette. Fig. 1 shows the appearance of a relaxed cardiac muscle cell attached to and internally perfused by means of a suction pipette. The internal perfusion caused little or no change in the microscopic appearance of the cell and its striations.

The image of one free end of the cell, which was bright compared with the background in phase-contrast microscopy, was projected onto the photodiode array (Fig. 3). A cylindrical lens was used to compress transversely the cell's image and the surrounding

---

FIGURE 2. (*opposite*) Verapamil-dependent and Cd^{2+}-dependent inward currents. (*A*) Voltage and time dependence of I_{si} before and 10 min after the addition of 100 μM verapamil. High-speed traces for a step to 0 mV are shown in the leftmost panel. Slower time base records for steps to different voltages before and after the addition of verapamil are shown in the middle and right panels. The voltages during the depolarizing steps were (top to bottom) −40, −20, and 0 mV in the top panel, and +80, +60, +40, and +20 mV in the lower panel. The vertical calibration bars (0.5 nA) show the zero-current level (horizontal line). Below are the current-voltage (*I-V*) curves for the peak inward current (solid symbols) and at 300 ms after the voltage step (open symbols) before (circles) and after (squares) the addition of verapamil. Data for voltages between −50 and −90 mV are for holding currents. Note that there was a change in these holding currents between the two measurements, but not in the resting membrane potential (zero-current intercept). This could be explained by a decrease (~30%) in the background K^+ conductance and would slightly decrease the amplitude of the verapamil-sensitive inward current measured for voltage steps to greater than −40 mV (see below). The traces in *A* are signal averages of four depolarizations. (*B*) A comparison of the verapamil-sensitive inward current (circles) with the magnitude of the time-dependent inward current $I_{peak} - I_{300}$ (triangles). The verapamil-sensitive current was obtained by digitally subtracting the currents after the addition of verapamil from those before its addition. $I_{peak} - I_{300}$ was measured from the *I-V* curves in *A*. The amplitude of the voltage steps is the same as in *A*. For voltage steps to 0 and +10 mV, the inward current peaked ~9 ms after the voltage step. The values for the peak verapamil-sensitive currents for voltage steps to above 0 mV are estimated (open circles) as the value of the current 9 ms after the voltage step, because of possible inaccuracies in our data recording system (FM tape) soon after the capacitative transient and because of early current transients sometimes seen in the digitally subtracted records during large voltage steps (see below). (*C*) A similar comparison for another cell in which the Ca^{2+} channels were blocked with 100 μM Ca^{2+}. The leftmost panel shows rapid time base records, for a step to 0 mV, of the currents before and after the addition of Cd^{2+}. The middle panels show high time base records of the digitally subtracted Cd^{2+}-sensitive currents. The voltages during the depolarization were (top to bottom) −40, −20, −10, and 0 mV for the upper panel, and +80 to +10 mV in 10-mV increments for the lower panel. Note the existence of a small inward-going transient ~5 ms after large voltage steps. The right-hand panel compares the Cd^{2+}-sensitive current (circles) with $I_{peak} - I_{300}$ (triangles), as in *B*. This experiment was performed in two cells. The traces in *C* are signal averages of three depolarizations.

phase halo in order to enhance the contrast between the cell and the background. The video signal representing the free end of the cell was compared with an adjustable threshold. A voltage step of fixed amplitude was (*a*) triggered to occur when the light intensity exceeded the threshold and (*b*) integrated to provide a linear ramp. The amplitude of the integrator output was sampled and held at the end of each scan. Since

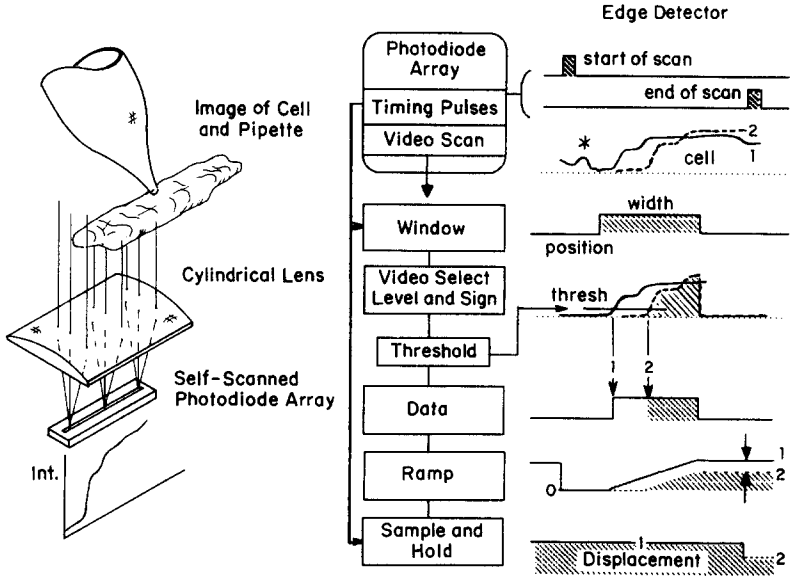

FIGURE 3. Method for measurement of contractile shortening. (*Left*) A schematic representation of the projection of the image of a cell through a cylindrical lens and onto a photodiode array. The intensity trace at the bottom ("Int.") gives light intensity as a function of position on the photodiode. (*Right*) A block diagram of the length-follower. Timing pulses trigger the scanning of the array 1,000 times/s. A window of variable size and position is adjusted to include one end of the cell and exclude unwanted signals from debris (asterisk). A threshold level ("thresh") is then manually set to the area of maximum slope on the video signal. A voltage step is then triggered and integrated whenever the video signal exceeds the preset threshold within the window. The final amplitude of the resulting ramp is sampled and held at the end of the scan. Note that as the cell shortens (position 1 to 2), the length of the free end of the cell and the amount of the array for which the light intensity exceeds threshold both decrease. The amplitude of the ramp at the far end of the video window will thus follow displacement of the end of the cell.

the integrator output was reset to zero at the beginning of each scan, the output voltage of the edge detector was directly related to the amount of the array covered by the cell's image. When the cell shortened (with its moving edge perpendicular to the long axis of the detector; Fig. 3, images 1 and 2), its image covered less of the detector and the output voltage (which was sampled and held) decreased. Thus, the position of the edge of the cell could be computed 1,000 times/s.

The ends of unattached heart cells shortened freely about a central point when stimulated to contract by extracellular electrodes (as described above). The ends of voltage-clamped, internally perfused cells shortened toward the stationary suction pipette attached

to the center of the cell. In both cases, the number of sarcomeres (N) in the free end of the cell projected onto the photodiode was counted. The resting sarcomere length (SL_0) in this free end of the cell was measured (as the average of at least 10 striations) with a filar micrometer, which had been calibrated against a 10-μm grating. We could then relate changes in the output voltage of the length-follower (ΔV) to sarcomere length (SL) by the formula

$$SL = SL_0 - K\Delta V/N,$$

where K is the constant relating distance to voltage for the length-follower as measured from the image of a 10-μm grating.

This calculation assumes that the sarcomeres in the unattached part of the cell shorten uniformly; otherwise, there would be a spread of sarcomere lengths, and this formula would give only an average sarcomere length for the unattached end of the cell. We visually inspected and recorded the striated appearance of the sarcomeres during the contractions with the television system to determine whether or not they contracted uniformly.

As a first approximation, the limiting resolution of displacement of a perfect edge is determined by the ratio of the length of an object whose projected image would cover the array and the number of elements in the array (i.e., 75 μm/256 elements = 0.3 μm/element). In practice, the length-follower could detect edge displacements as small as 0.2 μm, as estimated by knowing (*a*) the total voltage changes associated with the fixed displacement of a calibration grating in the microscopic field of view and (*b*) the minimum detectable changes in the voltage output. Inasmuch as the free ends of the cell usually contained >30 sarcomeres, this is equivalent to a measurement precision of better than 0.01 μm/sarcomere, or 0.5%. Some cells had up to 60 sarcomeres in the free end, and the precision of measurement was improved accordingly.

In general, the peak velocity of shortening and the maximum amount of shortening in a cell changed in a parallel manner. The former, however, occurred soon after depolarization, and it was therefore less affected by the additional shortening that occurred upon repolarization of the cell after large depolarizations (see Results). Therefore, we chose to use the peak velocity of shortening during the depolarization step (V_{peak}) as a quantitative measure of contraction. V_{peak} was determined by hand as the tangent of the sarcomere length traces.

Experimental Protocol

The ventricular cells isolated from the guinea pig were irregular in shape and highly variable in size. The cells used in our study ranged from 95 to 180 μm in length and from 15 to 30 μm in width. All of the cells chosen for study were roughly rod-shaped, had no visible surface blebs, and had resting sarcomere lengths of $\geq$1.80 μm/sarcomere. For voltage-clamp experiments, only cells that maintained a stable outward current at a holding potential of −50 mV were used.

Cell pairs and larger multicellular aggregates were excluded from this study. We could distinguish multicellular preparations by their optical appearance and also by their contractile behavior. We voltage-clamped one cell of a cell pair on three occasions (twice intentionally). The extent and time course of shortening differed significantly in the two cells. This was not surprising, because only the cell that was attached to the pipette would be internally perfused at a rapid rate and reliably voltage-clamped.

After membrane rupture, the holding potential was usually set to −50 mV. This, along with the TTX, should have eliminated the fast Na^+ current. The cell was then depolarized to 0 mV in steps lasting 300 ms, 30 times/min, until the contractile shortening and current

stabilized (usually within 1 min). The shortening seen under these stimulus conditions will be known as steady state control shortening.

The extent of shortening and the amplitude of the peak inward current gradually decreased as a function of time after the onset of internal perfusion, under the same stimulus conditions (see Results). When the change during an experimental protocol was significant, the values of the peak current and of the shortening velocity were normalized to those of steady state control contractions interspersed throughout the experiment.

Under certain conditions (e.g., high stimulus frequencies, long depolarizations), some cells developed aftercontractions (i.e., spontaneous and asynchronous sarcomere shortening, which followed the stimulated twitch; see Mitchell et al., 1985). Data from cells under these conditions were excluded from this study.

All experiments were performed at room temperature. Unless otherwise noted, the extracellular [Ca^{2+}] was 2.5 mM, the stimulus rate was 30/min, and the depolarization step duration was 300 ms. The microscopic appearance of the contracting cell and its striations were recorded on videotape (SL-2710 Sony, Tokyo, Japan). The membrane potential, currents, and cell length were stored on FM tape for analysis (A. R. Vetter Co., Rebersburg, PA). Current traces were filtered at 1 kHz. Cell length traces were filtered at 100 Hz. Some traces were signal-averaged (TN-1505, Tracer Northern, Middleton, WI) to reduce noise.

For this study, voltage clamp, internal perfusion, and cell length measurement were successfully established on 18 cells. Unless otherwise noted, each of the complete experimental sequences reported was performed on at least three different cells, and all yielded comparable results. Data from multiple cells are expressed as means ± standard deviation (SD).

RESULTS

General Contractile Behavior of the Voltage-Clamped, Perfused Cells

The cells selected for study were, on the average, 120 μm long by 20 μm wide. They were quiescent during the intervals between depolarizations and had resting sarcomere lengths of 1.87 ± 0.03 μm (n = 14). This value did not change after the onset of internal perfusion. Steady state control depolarization from the holding potential to 0 mV elicited an inward current and twitch shortening (Fig. 4). Shortening appeared to be uniform and synchronous throughout the unattached parts of the perfused cell. The times from stimulation to the onset and to the peak of shortening, 40 ± 16 and 308 ± 76 ms, respectively (n = 15), compared favorably with the values of 41 ± 12 and 349 ± 52 ms (n = 10) obtained with unattached, nonperfused cells stimulated at the same rate. These similarities suggest that the steps that initiate the release of Ca^{2+} from the internal stores are unaltered by the intracellular perfusion technique.

The extent and velocity of shortening of both the intact, electrically stimulated cells and the perfused, voltage-clamped cells varied from cell to cell. Some cells shortened vigorously, while others shortened only a small amount (compare, e.g., Figs. 4, 6, and 7). The extent of shortening decreased by an average of 45% in the three cells in which we measured shortening both before and after the onset of internal perfusion (cells stimulated 30 times/min with 300-ms voltage-clamp steps from −50 to 0 mV, 1–1.5 min after the onset of internal perfusion). We would expect the perfused cells to shorten less than intact cells, because of

the increased Ca^{2+} buffering of the perfusate. In any case, the results we describe below are independent of the extent of shortening.

Electrical Characteristics of the Voltage-Clamped Cells

The resting membrane potential (from the zero-current crossover in voltage clamp) of a subset of the cells in this study was −65 ± 4 mV (n = 9). The

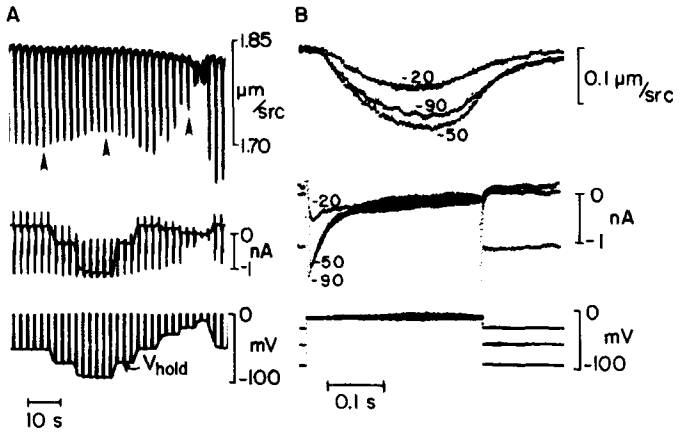

FIGURE 4. The effect of the holding potential on twitch shortening. (*A*) A slow time base recording of sarcomere length (top), membrane current (middle), and membrane potential (bottom), while the holding potential (V_{hold}) was varied between −90 and −10 mV. Contractions were triggered by 300-ms depolarizations to 0 mV. All traces for slow time base recordings such as these were filtered at 30 Hz. For the current traces, the large downward deflection is the slow inward current (I_{si}), and the smaller downward and the upward deflections are the capacitative artifacts. Note that when V_{hold} was more positive than −20 mV, there was some generalized shortening of the cell. (*B*) Contractile shortening, currents, and membrane potential for the three contractions marked with arrowheads in *A*, at a faster time base. The numbers near each trace indicate the holding potential from which depolarization was triggered. To facilitate a comparison, the sarcomere length traces for the three contractions have been repositioned so as to appear to start from the same initial length. Note that the inward current following a voltage step from −90 to 0 mV was larger and peaked somewhat sooner than a voltage step from −50 to 0 mV. This probably represents some residual Na^+ current through the fast Na^+ channels at a holding potential of −90 mV.

calculated K^+ equilibrium potential was −75 mV, given an intracellular [K^+] of ~108 mM and an extracellular [K^+] of 6.0 mM. Thus, the membrane is fairly selective for K^+. The input resistances for these cells (for voltage steps to −90 mV) ranged from 13 to 80 MΩ (mean, 36 MΩ).

The survival time of the cells after the onset of internal perfusion ranged from a few minutes to over an hour. We saw a time-dependent decay of the peak Ca^{2+} current (Fig. 8*B*, contractions 1 and 5), as reported by others for the internally perfused heart cell (Lee and Tsien, 1982; Irisawa and Kokubun, 1983). This

progressive decrease in I_{si} was always accompanied by a decrease in sarcomere shortening. The twitch shortening in response to depolarizing steps eventually disappeared in most cells. Thus, in intact isolated cells, a small or absent contractile response to external stimulation may reflect a decreased number of functional Ca^{2+} channels.

In some cases, however, the cells began to contract spontaneously and asynchronously. This usually accompanied a decrease of the cell's input resistance, and probably signified a breakdown of the high-resistance seal between the cell and the pipette. This was followed by a progressive decrease in the mean length of the cell.

Alterations of the Holding Potential

Fig. 4 shows the effect of changes in the holding potential on steady state twitch shortening caused by voltage steps to 0 mV. Hyperpolarizing the cell (from −50 to −90 mV) slightly decreased the magnitude and velocity of the steady state shortening, with only minor changes in the time course of the inward current (Fig. 4*B*). Holding potentials more positive than −40 mV decreased both the inward current and the twitch shortening. Upon the return of the holding potential to −50 mV, however, the shortening (but not the inward current) was temporarily enhanced.

The relationship between steady levels of depolarization and the sarcomere length for a nonstimulated cell is shown in Fig. 5. As also shown in Fig. 4*A*, changes in the holding potential between −90 and −50 mV did not significantly alter the resting sarcomere length. For holding potentials more positive than −40 mV, however, we saw considerable generalized shortening of the cell. This shortening was greater at more positive potentials, up to and exceeding +100 mV, which is near the Ca^{2+} equilibrium potential. The shortening was also seen in the presence of 100 μM Cd^{2+} (two experiments). Thus, an influx of Ca^{2+} through membrane Ca^{2+} channels is probably not responsible. The cell relengthened (although not fully) and again became quiescent when it was repolarized. If the depolarization was maintained at large voltages, however, the shortening progressed and became irreversible; the cell then became rounded and its striated pattern was lost.

This shortening was accompanied by nonuniform oscillations of sarcomere length (Fig. 5). We could not determine an obvious focus of origin for these contractile waves, and there were often multiple waves in a cell at any given time. Thus, we were unable to quantify the frequency of these oscillations. The voltage at which this spontaneous shortening began was somewhat variable from cell to cell, and a small amount of steady slow shortening was usually visible before the oscillations began (for steady shortening, see Figs. 4*A* and 9). The oscillatory shortening of cell length was accompanied by very small oscillatory inward currents that decreased with increasing depolarization (Fig. 5).

Thus, the velocity and amplitude of the twitch shortening decreased immediately when a less negative holding potential decreased I_{si}. In addition, a period of sustained depolarization caused a slow, nonuniform oscillatory shortening that was independent of I_{si}. The sustained depolarization also potentiated future

control twitch shortening, whereas sustained hyperpolarization weakened twitch shortening.

Alterations of the Extracellular [Ca^{2+}]

We raised the extracellular [Ca^{2+}] around an internally perfused cell from 1.0 to 3.0 mM (Fig. 6*A*). The inward current (middle panel), the peak shortening velocity, and the amplitude of shortening (top panel) increased simultaneously. The time between depolarization and the onset of shortening decreased somewhat, but the overall time course of the contraction did not change significantly.

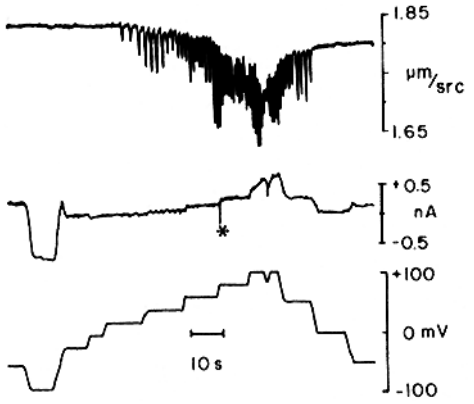

FIGURE 5. The effect of different holding potentials, without superimposed depolarizing steps, on sarcomere length and membrane currents. The shortening was spontaneous and nonuniform throughout the cell, with multiple foci of contraction. For this reason, the listed sarcomere length is an average of the lengths of all the sarcomeres in the free end of the cell projected onto the photodiode, and not the length of any given sarcomere. Note that the cell did not relengthen fully after repolarization. The asterisk denotes a region of damage on the FM tape.

For comparison, the effect of an increase in [Ca^{2+}] on an intact, nonperfused, electrically stimulated heart cell is shown in Fig. 6*B*. Here, the time between stimulation and the onset of rapid shortening decreased, the amplitude and velocity of shortening increased, and relengthening was accelerated.

Alterations of Frequency of Stimulation

Fig. 7 shows the effect of a change in the stimulus rate on shortening in an internally perfused, voltage-clamped single heart cell (Fig. 7*A*), and in an intact, nonperfused heart cell stimulated to contract by an extracellular electrode (Fig. 7*B*). In both cases, an increase in the frequency of stimulation (to a point) caused an increased amplitude and velocity of shortening that developed gradually over the course of several contractions. In the perfused cell, the peak inward current with each depolarization and the time course of contraction were not significantly affected by the stimulus rate (Fig. 7*A*). The velocities of shortening and relengthening increased in parallel. In contrast, the contraction of the nonperfused intact

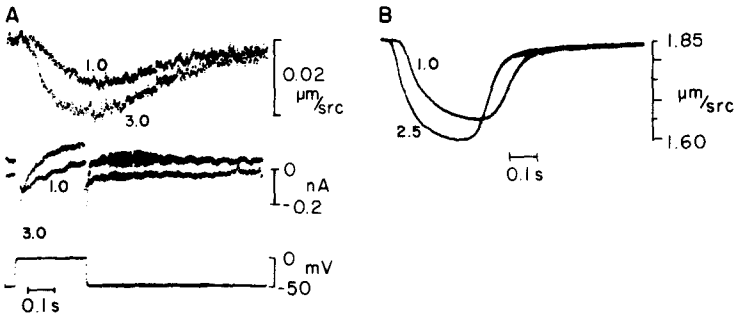

FIGURE 6. The effect of raising the extracellular [Ca^{2+}] on contraction. (*A*) For this internally perfused cell, the extracellular [Ca^{2+}] was raised from 1.0 to 3.0 mM The resting sarcomere length was 1.9 μm/src. The sarcomere length and current traces were all recorded under steady state conditions and are signal averages of four contractions. This experiment was performed on two cells. (*B*) For this intact cell, the extracellular [Ca^{2+}] was raised from 1.0 to 2.5 mM. The sarcomere length traces were recorded under steady state conditions and are signal averages of eight contractions.

cell was markedly abbreviated by increased stimulus frequencies (Fig. 7*B*); this change was evident on the first contraction at the new rate. In addition, increased stimulus frequencies markedly shortened the delay from stimulation to the onset of rapid sarcomere shortening only in the intact, nonperfused cell. For very low stimulus frequencies, a very slow phase of sarcomere shortening was apparent (Fig. 7*B*, inset); this made the determination of the true mechanical latency difficult.

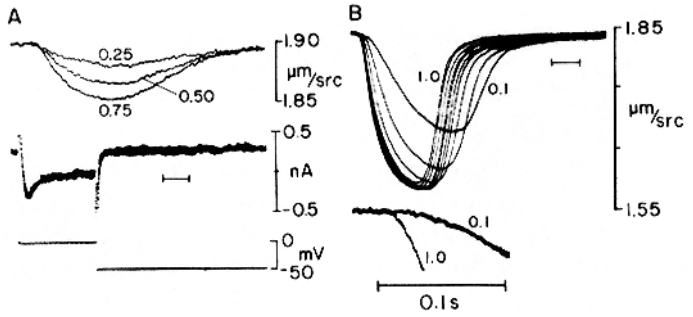

FIGURE 7. The effect of increasing the rate of stimulation on contraction for a voltage-clamped, perfused heart cell (*A*) and for an intact, nonperfused heart cell (*B*). The traces were taken under steady state conditions and are signal averages of 4 (*A*) and 10 (*B*) contractions. The stimulus rates (in hertz) are given next to each trace in *A*. In *B*, the rate was increased from 0.1 to 1.0 Hz in 0.1-Hz increments. The sarcomere length traces were repositioned so as to appear to start from the same initial length. In actuality, there was some incomplete relengthening (<0.01 μm/src) at high rates of stimulation. The horizontal calibration bars are all 0.1 s. The inset in *B* shows at a faster time base the onset of shortening in this cell with a stimulation frequency of 1.0 Hz, and the slow phase of early shortening seen only in nonperfused cells stimulated at low rates.

In summary, for the perfused cell, a slow increase in the amplitude and velocity of shortening was associated with (*a*) more frequent depolarizations and (*b*) an increased net inward Ca^{2+} current (because I_{si} remained the same for each depolarization while the number of depolarizations per minute increased). Other experiments explored whether increased depolarization or increased integrated inward currents were associated with slowly increasing contractility under other conditions (see below).

Alterations of Voltage Step Amplitude

We changed the amplitude of the depolarizing step for 6–10 consecutive contractions. Fig. 8*A* shows a slow time base recording of one such sequence in which the depolarizing step amplitude was raised from the control value of 0 mV to +50 mV. Fig. 8*B* shows cell length, transmembrane current, and membrane potential for five of these contractions. Note that the dynamics of contractile shortening changed immediately as the depolarizing step was altered (contractions 1–2 and 3–4). The speed and amplitude of shortening continued to change at the respective depolarizing steps until a steady state was reached several contractions later (contractions 3 and 5). The currents, in contrast, changed when the voltage step was altered and remained constant thereafter (see, e.g., Fig. 9).

Any protocol for studying the influence of depolarization on contraction must account for both these immediate and slower adjustments in contractility. We describe first the immediate changes that occurred when the depolarizing step amplitude was altered. The gradual adjustments that followed are discussed afterwards.

Rapid changes in contractility. Fig. 8*C* summarizes the effect of eight different changes in the voltage step amplitude on the inward current (I_{si}, dashed line) and on the peak velocity of shortening (V_{peak}) of the first contraction at the new voltage (solid line, open circles). Depolarizing steps to less than the control value of 0 mV activated less inward current and resulted in an immediate reduction of V_{peak}. Depolarizing steps to above 0 mV also decreased both I_{si} and V_{peak}. Steps to above +70 mV, the apparent reversal potential for Ca^{2+} (Lee and Tsien, 1982), always eliminated the uniform, synchronized twitch shortening during depolarization (n = 10; Fig. 9). There is therefore a good correlation between the peak inward current and the maximum velocity of shortening (Fig. 8*D*).

When the duration of depolarization was longer than 300 ms, very large voltage steps caused a slow shortening with superimposed asynchronous contractions. This was similar to the nonuniform, asynchronous shortening seen with large positive holding potentials, as in Fig. 5.

With large voltage steps (Fig. 9 and Fig. 10*B*, contraction 2), we saw a uniform late shortening of variable amplitude, the onset of which followed repolarization to the holding potential and the associated inward-going tail current. This tail current resulted in part from an inward Ca^{2+} flux through noninactivated Ca^{2+} channels (Isenberg and Klockner, 1982). Thus, a uniform, synchronized twitch contraction followed two very different inward Ca^{2+} currents: the I_{si} associated with depolarization and the tail current associated with repolarization. Moreover,

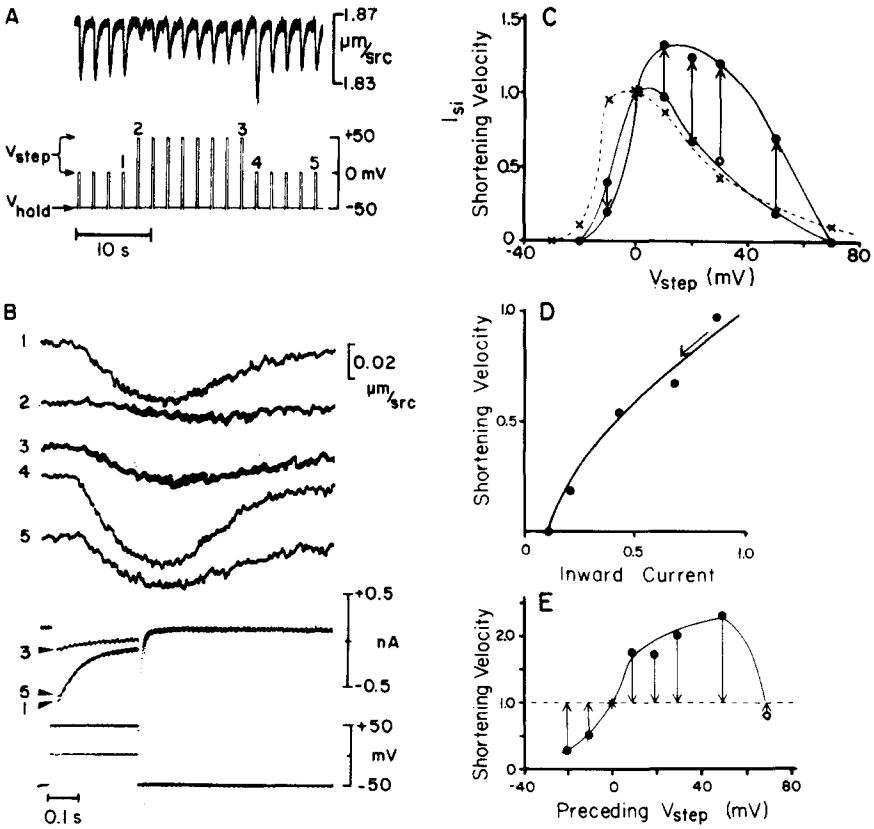

FIGURE 8. (*A*) The effects of changing the amplitude of the depolarizing step (V_{step}, bottom panel) on contractile shortening (top). V_{step} was changed from 0 (steady state control) to +50 mV and back to 0 mV. The holding potential, V_{hold}, was −50 mV. (*B*) Contractile shortening (top), transmembrane current (middle), and membrane potential (bottom) for five of the contractions in *A*. The shortening traces were filtered at 50 Hz. The current traces are signal averages of four steady state contractions. Note that the peak inward current and shortening in contraction 5 are both slightly smaller than in contraction 1, which indicates a rundown of the cell during the 30 s between them. (*C*) The effect of eight different changes of V_{step} on I_{si} (measured as $I_{300} - I_{peak}$, ×) and on the peak velocity of shortening (V_{peak}) of the first contraction (○) and of the steady state (●). At any V_{step} (e.g., contraction 3 in *B*), I_{si} and V_{peak} (during the depolarizing step) were normalized by the average of the respective values, which occurred in the preceding and following series of steady state voltage steps to 0 mV (e.g., contractions 1 and 5 in *B*). The arrows indicate the change in the shortening velocity between the first and the steady state contraction at the indicated voltage. (*D*) V_{peak} of the first contraction at a new depolarizing step as a function of I_{si} at that depolarizing step, for $V_{step} > 0$ mV. Data were normalized as in *C*. The arrow indicates the direction of increasing depolarizing step amplitude. For $V_{step} < 0$ mV, the time course of the inward current differed from that with larger steps, and V_{peak} was more variable from cell to cell. (*E*) The effect of prior depolarizations on contraction. The V_{peak} of the first contraction after the return of the depolarizing step from each V_{step} to 0 mV is shown (e.g., contraction 4 in *B*). The velocity was normalized against the following steady state control step to 0 mV (e.g., contraction 5 in *B*), and the arrows indicate the direction and magnitude of the change to steady state. Note that for depolarization to +70 mV (open circle), contraction accompanied repolarization and not depolarization.

the late shortening demonstrates that the intracellular Ca^{2+} release process could proceed in the absence of membrane depolarization.

The delay between the repolarization and the onset of shortening (following the large voltage steps) was as much as 20 ms shorter than the delay between depolarization and the onset of shortening (under conditions where depolarization triggered I_{si} and contraction) in the same cells.

Aside from this shortening associated with repolarization (which delayed relengthening after large voltage steps), alterations in the amplitude of the depolarizing steps did not significantly affect the time course of shortening. The

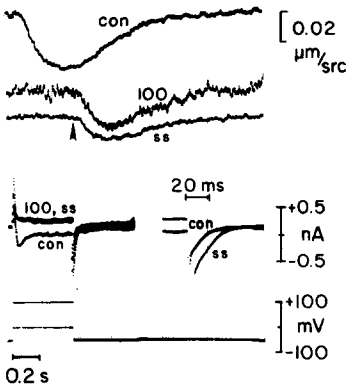

FIGURE 9. The effect of a large depolarization on the shortening (top) and currents (middle). The traces labeled "con" represent a steady state control contraction (a depolarization from −50 to 0 mV). The traces labeled "100" represent the first contraction with a voltage step to +100 mV, and the traces labeled "ss" represent a steady state contraction at that voltage step. The duration of the voltage step was 475 ms. Length traces for "con" and "ss" are signal averages of four contractions. The arrowhead beneath the length traces indicates the onset of repolarization. Note that the current traces for the first and the steady state contractions with a voltage step to +100 mV superimpose. Also note that there is a small amount of steady shortening ~300 ms after the step to 100 mV. The inset shows the tail currents (capacitative artifact not removed) that followed repolarization. Although other currents are probably responsible (e.g., an electrogenic Na/Ca exchange), at least part of the tail current represents Ca^{2+} flowing into the cell through noninactivated Ca^{2+} channels. Same cell as in Fig. 7*A*.

time between stimulation and the onset of shortening was longer with very small voltage steps (to less than −10 mV), however.

Slow adjustments in contractility. The amplitude of the depolarization also influenced the difference between the peak velocity of shortening of the first contraction at a new voltage and the steady state at that voltage (Fig. 8*C*, arrows between open and solid circles). Decreasing the voltage step amplitude from the control value of 0 mV resulted in a gradual decrease in the velocity and amplitude of shortening, whereas increasing the voltage step amplitude increased the shortening over the course of several contractions. Similarly, upon the return of the depolarizing step to 0 mV (control), the size of the first contraction depended

in a predictable way upon the amplitude of the preceding voltage steps (e.g., Fig. 8*A*, contraction 4 vs. 5). A series of small depolarizing steps (to less than 0 mV) depressed the first few control contractions that followed, whereas a series of large depolarizing steps (to between 10 and 50 mV) enhanced the subsequent control contractions (Fig. 8*E*). Thus, larger voltage steps caused a slow increase in the amount and speed of shortening, despite the fact that the inward currents (peak and integrated; Fig. 2) during depolarization were reduced from the control conditions.

Alterations of Voltage Step Duration

Very brief depolarizations (i.e., those that ended well before the peak of the inward current and presumably did not trigger a large Ca^{2+} tail current) either (*a*) immediately decreased the peak velocity and extent of shortening or (*b*) eliminated shortening entirely. Changes in the duration of depolarization that did not encroach on the peak inward current (i.e., to voltage step durations >40 ms) affected total shortening but had no effect on the maximum velocity of shortening of the first contraction at the new step duration (Fig. 10*A*, contraction 2). Thus, the events that determine the initial phase of contractile shortening occur near the beginning of the voltage step.

The cell shortening gradually adjusted to a new steady state level after a change in the duration of the depolarizing step (Fig. 10, *A* and *B*). Longer depolarizations increased the maximum velocity of shortening at the steady state (Fig. 10*C*), with no change in the peak inward current. This was true even with voltage steps to +60 mV (Fig. 10, *B* and *C*), for which the inward Ca^{2+} current was much smaller. Thus, alterations of the duration of the depolarizing step were associated with a slow change in contractility; this change occurred without any change of the peak inward current and did not depend on the size of those currents.

Lengthening depolarization prolonged shortening and delayed relengthening (Fig. 10*D*). This effect occurred as soon as the duration of depolarization was altered (contraction 2 of Fig. 10, *A* and *B*) and before the gradual change in the peak shortening velocity had occurred. Relengthening did begin before the end of long depolarization steps (Fig. 4*B*), although it was always incomplete. Conversely, there seemed to be a minimum possible duration of contraction, seen with depolarizations of <100 ms. Moreover, when repolarization from a voltage step to +100 mV triggered shortening (Fig. 9 and Fig. 10*D*, asterisk), contractile duration was also at that minimum value. Here, shortening took place at the holding potential, and the voltage step duration was therefore effectively nil.

Microscopic Features of Contraction in Voltage-Clamped Heart Cells

In summary, two distinct types of shortening were apparent in the voltage-clamped cells. First, uniform synchronous shortening of the cell occurred in response to (*a*) depolarizations that triggered I_{si} (Figs. 4, 6*A*, 7*A*, 8, and 10) and/or (*b*) repolarization from large positive potentials (Figs. 9 and 10*B*). This pattern of shortening resembled the twitch of intact, nonperfused cells (Figs. 6*B* and 7*B*) and will be referred to as "twitch shortening." This type of contraction is probably the same as the "phasic" tension reported in multicellular voltage-clamp

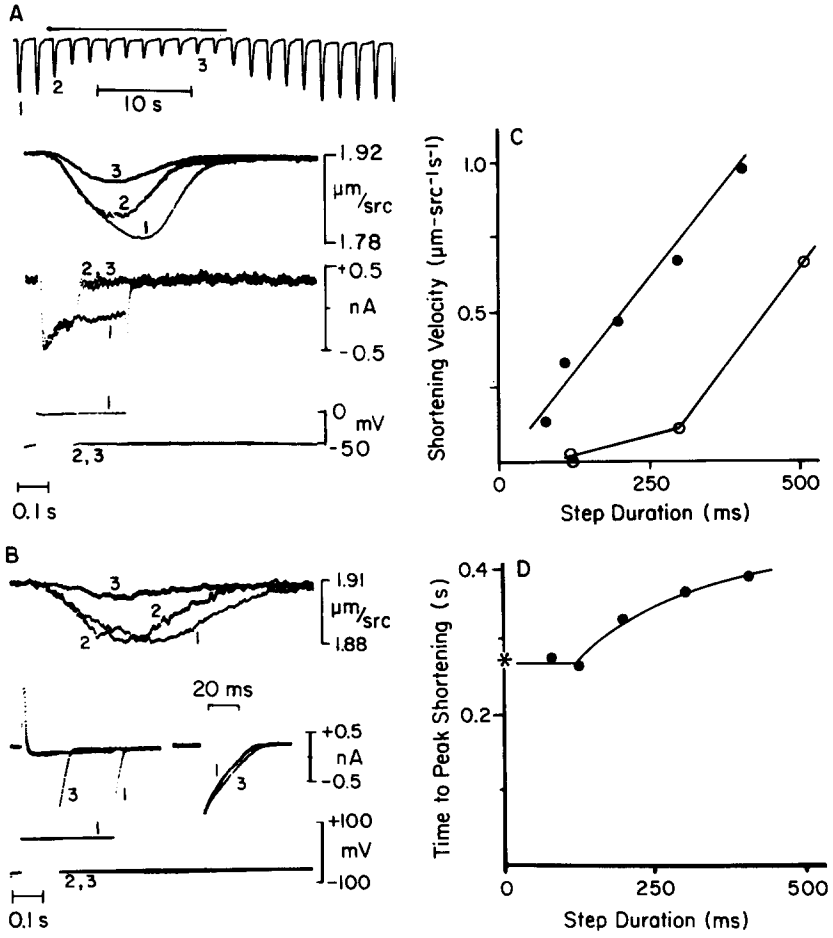

FIGURE 10. (*A*) The effect of decreasing the duration of the depolarization for 10 contractions. At the top is a slow time base recording of the sarcomere length; the horizontal bar indicates those contractions for which the duration of depolarizations was shortened. Length and current records for representative depolarizations are shown below. Contraction 1 is the steady state with a 300-ms depolarizing step (V_{step} = 0 mV), and 2 is the first and 3 the steady state with a 120-ms step. The length traces of contractions 1 and 3 are signal averages of the last four contractions with their respective voltage step durations. (*B*) The same sequence of changes in the duration of depolarization as in *A*, except that V_{step} = +60 mV. Note that the amount of shortening is smaller than in *A*, as is I_{si} (see, e.g., Fig. 8). Also note that there is additional shortening after repolarization of the brief depolarizations (trace 2). The inset shows the tail currents, which are smaller with the longer depolarization. (*C*) V_{peak} during depolarization as a function of depolarizing step duration, at steady state, for steps to 0 (solid circles) and +60 mV (open circles). (*D*) The time-to-peak shortening, at steady state, as a function of voltage step duration. The point at 0 ms (asterisk) was taken from shortening triggered by repolarization from V_{step} = +100 mV (Fig. 9). Note that when the duration of the voltage step was changed, the time course of the contraction changed immediately (e.g., in *A* and *B*). Same cell as in Fig. 7*A*.

studies (Chapman, 1983; Fozzard, 1977). Second, an oscillatory form of contraction with multiple foci of shortening occurred in response to (*a*) a holding potential above 0 mV (Fig. 5) and (*b*) long depolarizations of large amplitude (data not shown). This type of shortening could be considerably greater than that of the twitch, and was associated with an overall decrease of sarcomere length. Had the ends of the cell been held in place, a considerable amount of tension would have been expected. Thus, this type of nonuniform asynchronous shortening is probably the basis of the "tonic" tension reported in the multicellular voltage-clamp studies and probably has no analogue in the contraction of the intact heart.

DISCUSSION

The Internally Perfused, Voltage-Clamped Single Heart Cell

We have shown the feasibility of simultaneously measuring membrane currents and shortening in an internally perfused, voltage-clamped heart cell. Thus, E-C coupling can be examined under well-defined conditions in cells with intact membrane systems.

Inward currents. The slow inward current traces that we observed were similar to those reported in other studies in which the intracellular perfusate did not permit shortening and in which Ca^{2+} was the only permeant cation (Lee and Tsien, 1982, 1984). Thus, the motion of the cell does not disrupt the high-resistance seal between the cell and the pipette, or interfere with the electrical measurements in the isolated cells.

There are several potential difficulties with the measurement of the inward Ca^{2+} current in our system. (*a*) We measured the series resistance of the pipette in free solution and compensated for this value. The series resistance across the pipette tip may have been greater when it was attached to the cell, however (Irisawa and Kokubun, 1983). This would decrease the accuracy of the voltage clamp and cause an underestimation of the peak inward current. (*b*) The T-tubules in the guinea pig myocyte constitute a distributed series resistance across a part of the cell membrane. Thus, some nonuniformity in the voltage clamp is inevitable. (*c*) Our internal perfusate was more complex than those used in other electrophysiological studies. The composition of this solution was designed to support shortening, but the electrophysiological effects of its constituents have not been characterized fully. Thus, the use of this more physiological intracellular solution limits the certainty with which we can assign ions to the currents we observed. In particular, other voltage- and time-dependent currents were present in addition to the inward Ca^{2+} current (Fig. 2). (*d*) The motion of the cell limits our ability to perform certain other experiments. For example, the use of a second electrode at a distance from the first would result in tension development between the electrodes and disruption of the high-resistance seal(s).

Despite these concerns, we believe that this preparation yields an adequate voltage clamp and a good qualitative estimate of the inward Ca^{2+} current. The similarities of $I_{peak} - I_{300}$ and of the verapamil/Cd^{2+}-sensitive inward current over a wide voltage range support this conclusion (Fig. 2).

Cell length measurement. Contractile force is traditionally used to infer the amplitude of the cytoplasmic [Ca^{2+}] (and thus myofilament-bound Ca^{2+}). Tension has been measured on intact isolated mammalian heart cells (Fabiato, 1981; Brady et al., 1979). In our setup, however, the development of tension would probably disrupt the high-resistance seal between the suction micropipette and the cell.

A convenient method for the measurement of contraction in cardiac muscle preparations relies on changes in the light transmitted through the cells (Bucher, 1957; Boder et al., 1971). Related photoelectric techniques have been applied to individual cardiac cells (Mitchell et al., 1985; Fabiato and Fabiato, 1972). These methods are difficult to quantify, however, because of the absence of any simple and unique physical basis that relates shortening to the optical properties of the cell (Fabiatio and Fabiato, 1972; Clusin, 1981).

These difficulties do not exist if the edge of the cell is detected directly. Isenberg used a photodiode array to measure contractile shortening from the videotaped image of electrically stimulated (Isenberg, 1982) or voltage-clamped (Isenberg et al., 1985) single heart cells. Their temporal resolution was limited to 20 ms, however. We used a preset threshold to detect the position of the edge of the cell. Thus, changes in the optical properties of the cells during the contractile cycle did not affect the measurements. We also measured cell shortening directly from the microscopic image of the cell with a temporal resolution of 1 ms.

We used the peak velocity and extent of shortening as an index of changes in the peak intracellular [Ca^{2+}] during successive twitches. Maughan et al. (1978) studied the effect of [Ca^{2+}] on the peak isometric tension development and on the shortening velocity at any given load in skinned guinea pig ventricular muscles. They found that isometric tension and isotonic shortening velocity increased in parallel as [Ca^{2+}] was increased. Our single cells shortened freely, but a small internal load that opposes shortening must exist to explain why peak twitch shortening varies (Krueger et al., 1980). In addition, manipulations that are known to raise the peak intracellular [Ca^{2+}] in intact cells, such as catecholamines (Allen and Kurihara, 1980), also increase the shortening velocity (Isenberg, 1982). Thus, in the absence of factors that modify the sensitivity of the myofibrils to Ca^{2+}, changes in the peak cytoplasmic [Ca^{2+}] should cause parallel changes in the peak extent and velocity of shortening.

Internal perfusion. With the suction-pipette voltage-clamp method, the solution filling the pipette diffuses into the cytoplasm (Brown et al., 1981). The speed of the exchange depends on the diameter of the suction pipette and the size of the molecule in question. Measurements of the response of transmembrane currents to channel modifiers and to ion substitution have indicated that a new steady state is reached within several minutes (Lee and Tsien, 1984; Irisawa and Kokubun, 1983). We found, using pipettes with diameters of 2–8 μm, that rigor shortening began within 30 s after switching the perfusate to one lacking MgATP. In addition, the amplitude of the contractions stabilized within 1 min after the onset of internal perfusion. Thus, the exchange of small ions from the perfusate to the cell was reasonably rapid; moreover, sufficient ATP and/or CP

diffused into the cell to permit twitch contractions at rates up to at least the 45/min used in this study.

We weakly buffered the $[Ca^{2+}]$ in the intracellular perfusate to pCa 7. Clearly, cytoplasmic $[Ca^{2+}]$ increased considerably after stimulation. While the suction pipette should have tended to buffer the cytoplasm, we do not actually know its instantaneous or steady state composition; this is especially true for ions that rapidly move across the cell membrane, and for compounds that are synthesized or broken down intracellularly. Fortunately, we can infer changes in the peak intracellular $[Ca^{2+}]$ from changes in cell shortening.

The intracellular $[Na^+]$ in intact preparations increases with increased stimulation frequency (Cohen et al., 1982). The $[Na^+]$ in our experiments should have been much less variable, because of the intracellular perfusion and the blockade of the fast Na^+ channels by TTX. Thus, the changes in contractility in our perparation cannot be attributed to changes of the intracellular $[Na^+]$, which then caused changes in the intracellular $[Ca^{2+}]$ via the Na/Ca exchange.

Other studies have described shortening in isolated cardiac cells using one- and two-microelectrode voltage clamps (Mitchell et al., 1984, 1985; Isenberg et al., 1985), methods with which the intracellular milieu is more nearly physiological. Certain features of our results, such as the lack of any change in the peak inward current when the stimulus frequency was altered, probably reflect the effects of intracellular dialysis. For example, the phosphorylation state of membrane channels and contractile proteins probably varied less in our studies. Thus, a comparison of the results from these different methods should be instructive. Moreover, the suction pipette method will permit the role of specific intracellular constituents in contraction to be tested.

Relation to previous voltage-clamp studies. We emphasize that many of the results and conclusions reported in this study have been previously reported from multicellular voltage-clamp experiments (for reviews, see Chapman, 1983; Fozzard, 1977). However, there are conflicting data in the literature, and no single previous study has reported the entire range of results described here with our preparation. In addition, we have microscopically defined the nature of the phasic and tonic contractions of the previous studies. Thus, we have confirmed a number of previous experiments under conditions where the inadequacy of voltage control, heterogeneity of cell response, and interstitial ion accumulation should not complicate the results (Reuter and Sholz, 1977*a*; Fozzard and Beeler, 1975).

Role of I_{si} as a Trigger for Shortening

The existence of Ca^{2+}-induced Ca^{2+} release from the SR has been clearly demonstrated under physiological conditions in mechanically skinned mammalian heart muscle preparations (Fabiato, 1983). In addition, the potential importance of the Ca^{2+} influx to the contraction of intact heart muscle has long been appreciated (Chapman, 1983). We are unaware of any direct demonstration of the role of the Ca^{2+}-induced Ca^{2+} release process in a preparation with intact membranes, however.

We have found that I_{si} during depolarization was required for uniform,

synchronous twitch shortening in the internally perfused, voltage-clamped heart cell. Conditions that eliminated I_{si} eliminated twitch shortening (see also Gibbons and Fozzard, 1975; Trautwein et al., 1975; Leoty, 1974; Morad and Goldman, 1973; New and Trautwein, 1972; Ochi and Trautwein, 1971; Beeler and Reuter, 1970; Fozzard and Hellam, 1968). These conditions included very brief depolarizations, very small depolarizations below the threshold for the activation of I_{si} (Fig. 8*C*), a depolarized holding potential (Fig. 4), and Ca^{2+} channel blockers. In addition, our preparation tolerated voltage steps to well above the Ca^{2+} reversal potential (as high as +150 mV). We found that these large depolarizations always eliminated both the slow inward Ca^{2+} current and the twitch shortening during depolarization (Figs. 8, *C* and *D*, and 9). Under these conditions, shortening was associated with repolarization to the holding potential and the inward tail current (Figs. 9 and 10*B*; see also Leoty, 1974; New and Trautwein, 1972; Beeler and Reuter, 1970). At least a part of the tail current is carried by Ca ions through slow Ca^{2+} channels that were opened (but not inactivated) by the preceding depolarization. Thus, our results support the conclusions of the previous voltage-clamp studies on intact multicellular preparations: an inward Ca^{2+} current, and not depolarization per se, is essential for twitch shortening in cardiac muscle.

Isenberg et al. (1985) measured shortening in single voltage-clamped guinea pig and bovine myocytes. They reported a "slow component of contraction" with a holding potential near −50 mV and low stimulation frequencies, and a "fast component of contraction" with a more negative holding potential and stimulation at a faster rate. Voltage steps to near the Ca^{2+} reversal potential eliminated the slow component of contraction but not the fast component. This result does not necessarily conflict with the Ca^{2+}-induced Ca^{2+} release theory, however. The conditions Isenberg et al. used to elicit the "fast component of contraction" (i.e., no TTX, high-frequency steady state contractions not under voltage clamp, one voltage-clamped contraction with a 20-ms prepulse from −85 to −45 mV) may have substantially loaded the cell with Na^+. The large positive clamp potentials may have then caused Ca^{2+} entry into the cell via an electrogenic Na/Ca exchange (see below), which could have triggered the SR Ca^{2+} release. We saw nothing analogous to this "fast component of contraction" at any holding potential or stimulation rate. In our preparation, however, the fast Na^+ channels were blocked by TTX and the intracellular [Na^+] was controlled by internal perfusion.

The relationship between the influx of Ca^{2+} across the cell membrane during a contraction and the amount of Ca^{2+} needed to directly activate the myofilaments has been studied extensively (see Chapman, 1983; Fabiato, 1983). Some authors have speculated that the inward Ca^{2+} current is sufficient to activate the myofilaments directly (Isenberg et al., 1985; Isenberg, 1982; Bers, 1983; Leoty, 1974; Beeler and Reuter, 1970). Their calculations did not take into account the soluble and fixed intracellular Ca^{2+} buffers other than the myofilaments, however (Fabiato, 1983). Fabiato concluded that the measured inward Ca^{2+} fluxes were insufficient to activate the myofilaments directly in the presence of these buffers. In addition, Marban and Wier (1985) blocked Ca^{2+} release from the SR of canine Purkinje fibers with ryanodine. They found that the Ca^{2+}

transient and tension development were >95% diminished, without a decrease of the action potential plateau. Since the action potential plateau is in part a function of I_{si}, they concluded that most of the Ca^{2+} that activates the myofilaments comes from the SR, and not from Ca^{2+} that enters the cell during the twitch.

We perfused single heart cells with a known concentration of the soluble Ca^{2+} buffer EGTA, and can therefore calculate the minimum Ca^{2+} influx needed to raise the cellular [Ca^{2+}] a given amount. Because our internally perfused cells are quiescent, we can infer that the resting intracellular pCa is greater than or close to the value of 7.0 in the intracellular perfusate (Fabiato, 1985*a*; Fabiato and Fabiato, 1972). Ignoring intracellular diffusion, Ca^{2+} binding to the myofilaments, and Ca^{2+} buffers not in the intracellular perfusate, and assuming relatively rapid binding to the 0.5 mM EGTA internal perfusate, raising the intracellular [Ca^{2+}] from pCa 7.0 to pCa 6.0 (a [Ca^{2+}] that would activate the myofilaments directly) would require 0.26 mM Ca^{2+}. This would be equivalent to a sustained inward current of 15 nA for 100 ms in a cell 100 μm long and 20 μm in diameter (Fabiato and Fabiato, 1979; Fabiato, 1981) and exceeds the currents that we measured by a factor of at least 25. Thus, in our preparation with intact membranes, the simplest explanation of the results is that the inward Ca^{2+} current triggers a larger intracellular Ca^{2+} release. As such, our results constitute direct support for a Ca^{2+}-induced Ca^{2+} release mechanism in the contraction of the mammalian heart.

Role of I_{si} as an Immediate Determinant of Contractility

In addition to its role as a trigger for contraction, the amplitude of I_{si} also influences the size of an initial component of the Ca^{2+} transient (Wier, 1980), the magnitude of the phasic contraction in other voltage-clamped preparations (Gibbons and Fozzard, 1975; Trautwein et al., 1975; Leoty, 1974; Morad and Goldman, 1973; New and Trautwein, 1972; Beeler and Reuter, 1970), and the extent and speed of shortening in intact preparations (e.g., effect of catecholamines, Reuter and Sholz, 1977*b*). We found a parallel relationship between the amplitude of I_{si} and the magnitude of shortening when (*a*) the extracellular [Ca^{2+}] was changed (Fig. 6), (*b*) the Ca^{2+} current decreased (ran down) as a function of time (Fig. 8*B*), and (*c*) the amplitude of the depolarizing step was altered (Fig. 8, *A–D*). In particular, as the amplitude of I_{si} decreased at voltages near the Ca^{2+} reversal potential, the velocity and extent of shortening similarly decreased. One possible explanation for these results is that the inward Ca^{2+} current grades the fraction of Ca^{2+} release from the SR (McDonald et al., 1981; Trautwein et al., 1975; Gibbons and Fozzard, 1975; Morad and Goldman, 1973), as has been shown in studies on skinned cells (Fabiato, 1983). Alternatively, the amplitude of the Ca^{2+} current may affect the loading of the intracellular stores (Bass, 1976; Gibbons and Fozzard, 1975; New and Trautwein, 1972; Beeler and Reuter, 1970), with the releasable fraction remaining constant (an all-or-none release).

The velocity of shortening and the amplitude of I_{si} immediately changed in a parallel direction when we changed the depolarizing step amplitude over a range of voltages up to the Ca^{2+} reversal potential (Fig. 8*D*). Inasmuch as the changes

were evident so soon (i.e., <50 ms after the step amplitude was altered on the first non-steady state contraction), we conclude that we altered the Ca^{2+} release process and not SR Ca^{2+} loading. Thus, the amplitude of the Ca^{2+} current immediately grades the size of each and every contraction.

Voltage-clamp experiments on skeletal muscle have shown that contractile tension first increases and then reaches a plateau as the amplitude of the depolarizing step is increased (Caputo et al., 1984). Tension does not decrease with voltage steps that would greatly reduce or eliminate any Ca^{2+} currents. This is consistent with an E-C coupling process that involves a graded voltage-dependent Ca^{2+} release (Costantin, 1975; Endo, 1977; Schneider, 1981). Meanwhile, both tension and shortening correlate well with transmembrane Ca^{2+} currents in frog heart muscle (Leoty and Raymond, 1972). These cells are thought to lack an SR, and the Ca^{2+} currents are believed to be large enough to directly activate the myofilaments (Cleeman et al., 1984; Horackova and Vassort, 1976). We have also found a close relationship between transmembrane Ca^{2+} currents and shortening in mammalian cardiac muscle. Here, we believe that the inward Ca^{2+} current triggers an intracellular Ca^{2+} release, the size of which is graded by the magnitude of the current. Thus, in each of the above systems, the E-C coupling process allows direct and immediate control of the size of the contraction.

Slower Determinations of Contractility

Increases in the frequency (Fig. 7), amplitude (Fig. 8), and duration (Fig. 10) of the voltage step all increased the amplitude and velocity of shortening over the course of a few (four to six) contractions. Unlike the immediate changes described above, this gradual adjustment of contractility occurred while I_{si} remained constant. This phenomenon has been reported often in the literature (Gibbons and Fozzard, 1975; Leoty, 1974; Morad and Goldman, 1973; New and Trautwein, 1972; Ochi and Trautwein, 1971; Beeler and Reuter, 1970; Wood et al., 1969), and it has usually been attributed to a change in the Ca^{2+} loading of the SR. Specifically, one or more components of the inward Ca^{2+} flux through the Ca^{2+} channel (Fabiato, 1985*b*; Gibbons and Fozzard, 1975; Beeler and Reuter, 1970), the Na/Ca exchange (Sheu and Fozzard, 1982), and the sarcolemmal Ca^{2+}-ATPase (Sulakhe and St. Louis, 1980) have been implicated as major determinants of the cytoplasmic [Ca^{2+}] and of the amount of Ca^{2+} stored in the SR; the internally stored Ca^{2+} is then available to be released by the Ca^{2+}-induced Ca^{2+} release process.

Flux experiments with ^{45}Ca have demonstrated the existence of an ATP-dependent Ca^{2+} pump in cardiac sarcolemmal vesicles, which would remove Ca^{2+} from the cell (Caroni and Carafoli, 1980). This system has a lower transport rate than the Na/Ca exchange, however. In addition, there is no reason to believe that the Ca^{2+} extrusion of this pump should be inhibited at depolarized membrane potentials, where the electrochemical gradient of Ca^{2+} is decreased. Thus, although this system may aid in the removal of Ca^{2+} from the cell, it cannot explain the slow voltage-dependent changes of contractility we have observed.

The net influx of Ca^{2+} via I_{si} does not account for the slow changes in contractility in the internally perfused cell. The increased voltage step amplitude,

up to +50 mV, gradually potentiated shortening even though I_{si} decreased above +10 mV (Figs. 2 and 8, *C* and *E*); a similar result and conclusion have been previously reported (Ochi and Trautwein, 1971). An increased voltage step duration also gradually increased shortening; this increase was equally effective for steps to 0 and +60 mV, even though the inward currents during depolarization differed by a factor of 10 (Fig. 10, *A–C*). The influx of Ca^{2+} via the tail currents cannot explain these results, because the inactivation of Ca^{2+} channels is time dependent and the Ca^{2+} tail current will be smaller for depolarizations of longer duration (Isenberg and Klockner, 1982). Finally, more positive holding potentials potentiated future twitch contractions (Fig. 4*A*; Morad and Goldman, 1973) or caused a slow shortening of the cell (Fig. 5) in the absence of a slow inward current. Thus, the tonic tension reported by others with long voltage steps or ramp depolarizations (Trautwein et al., 1975; Morad and Goldman, 1973; Beeler and Reuter, 1970) probably reflects an extreme of the process by which the cardiac cell slowly alters its contractility. Here, the intracellular $[Ca^{2+}]$ is probably pathologically high and has triggered spontaneous release of Ca^{2+} from an overloaded SR (Fabiato, 1985*a*). In summary, the slow change in contractility must reflect a mechanism by which Ca^{2+} can become available to the SR for release, which (*a*) depends on the amplitude and duration of depolarization and (*b*) is unrelated to I_{si}.

It seems likely that an electrogenic Na/Ca exchange (more than two Na ions exchanged for each Ca ion) is responsible for the tonic contractions (Eisner et al., 1983) and for the slow changes in contractility. The tonic contractions that accompany long depolarizations are reduced in low-Na^+ extracellular solutions (Arlock and Katzung, 1985). The slow changes in contractility are abolished in low-Na^+ solutions, as is any effect of the duration of depolarization on contractile strength (Leoty, 1974; Beeler and Reuter, 1970; New and Trautwein, 1972). Thus, depolarization of the heart increases contractility, probably via an influx of Ca^{2+} accompanied by a net outward current.

Mitchell et al. (1984) noted that the amount of shortening decreased with voltage steps to +60 mV in the rat but not in the guinea pig. They suggested that the SR may be a more important source of Ca^{2+} in the rat. Our results emphasize the importance of the internal Ca^{2+} store (the SR) in the guinea pig, and the multiple factors that influence its Ca^{2+} release. For example, an increase of the voltage step amplitude tended to decrease shortening via a decrease of I_{si}, but to increase steady state shortening via an increase of the loading of the internal store with Ca^{2+} (Fig. 8).

Determinants of the Time Course of Contraction

The delay between stimulation and the onset of shortening depended on the magnitude and the time course of the inward current in the internally perfused cells. A larger I_{si} reduced the time between depolarization and the onset of shortening (Fig. 6*A*). Longer delays occurred for voltage steps of small amplitudes, where I_{si} is smaller and its onset is slower (Lee and Tsien, 1982). Similarly, the onset of shortening followed a tail current more rapidly than it followed depolarization. In this case, we could not measure the magnitude of the peak

inward Ca^{2+} current; the Ca^{2+} influx during the tail current may have been greater than during I_{si}. In addition, the peak current should have occurred almost immediately after the voltage step back to the holding potential, because any delay required for the opening of the Ca^{2+} channels would have been eliminated. Thus, the size and time course of the Ca^{2+} current determine the timing of the onset as well as the size of the release of Ca^{2+} from the SR.

The duration of the contraction depended on the duration of the voltage step in the internally perfused, voltage-clamped heart cell. For brief voltage steps, there was a minimal contractile duration; otherwise, longer voltage steps prolonged shortening and delayed relengthening (Fig. 10). Relengthening was incomplete until the cell was repolarized. Similar effects of action potential duration on contractile duration have been reported previously (Wood et al., 1969; Morad and Trautwein, 1968). Since the cytoplasmic Ca^{2+} falls very rapidly (within 100 ms) after the depolarization (Wier, 1980), and the onset of relengthening can occur before repolarization (Fig. 4*B*), we believe that prolonged depolarization slows the removal of the Ca^{2+} from the myofilaments via the cytoplasm, as opposed to prolonging the Ca^{2+} release process. Indeed, the time course of shortening seems fairly independent of the membrane potential at which internal Ca^{2+} release occurs (Fig. 9). Thus, one possibility is that depolarization inhibits Ca^{2+} efflux from the cell via an electrogenic (or voltage-dependent) Na/Ca exchange, thereby prolonging contraction with long depolarizing steps and also loading the SR.

The overall time course of contraction depended only on the duration of the depolarization in our preparation (Figs. 4*B*, 6*A*, 7*A*, and 8). Thus, in any given cell, the amplitude of shortening at any time after depolarization scaled for contractions of vastly different sizes. This suggests that the amount of Ca^{2+} released into the cytoplasm does not affect the time course of contraction and relaxation in the dialyzed cell.

In intact, electrically stimulated cells, higher extracellular Ca^{2+} concentrations (Fig. 6*B*) and higher stimulation frequencies (Fig. 7*B*) abbreviated the time course of contraction. Higher stimulation frequencies also decreased the delay between stimulation and the onset of rapid shortening (Fig. 7*B*; refer to "slow" type of shortening of Isenberg, 1982). The discrepancy between intact and perfused cells may have resulted in part from control of the duration of depolarization in the voltage-clamped cells; an increased stimulation frequency and an increased extracellular $[Ca^{2+}]$ tend to decrease the action potential duration in intact isolated guinea pig heart cells (Nordin, C., and R. Aronson, personal communication). Moreover, because our preparation was internally perfused, the condition (e.g., the phosphorylation state) of the intracellular proteins was probably more constant. This may explain why the frequency dependence of the onset of contraction is seen only in the intact, nonperfused cell.

Application to the Intact Heart

The shape of the cardiac action potential varies under both physiologic and pathological conditions because of changes in the underlying ionic currents (Keung and Aronson, 1981; Fozzard, 1977). Our results suggest that, in the

intact heart, an increased slow inward current would increase the fraction of SR Ca^{2+} that is actually released into the cytoplasm. This would strengthen contraction without a direct effect on SR Ca^{2+} accumulation or on the time course of contraction. In addition, within the physiological range, an increase in the action potential duration or overshoot would augment internal Ca^{2+} release, independently of the inward current. Longer action potentials would also prolong contraction. Thus, a mechanism also exists by which prolongation of the cardiac action potential, as during hypertrophy (Keung and Aronson, 1981), would directly promote an increase in contractile strength.

We would like to thank Drs. E. H. Keung, D. C. Spray, C. Nordin, and E. H. Sonnenblick for their helpful advice, and Dr. Ira Cohen for a critical reading of the manuscript. We would also like to thank Ms. Nadine Stram and Mr. Robert Smith for their technical assistance.
This work was supported (in part) by National Institutes of Health training grant T32 GM 7288 from the National Institute of General Medical Sciences (B.L.), HL18824, HL21325, and by an Established Fellowship from the New York Heart Association (J.W.K.).

Original version received 5 August 1985 and accepted version received 4 June 1986.

REFERENCES

Allen, D. G., and S. Kurihara. 1980. Calcium transients in mammalian ventricular muscle. *European Heart Journal.* 1:5–15.

Arlock, P., and B. G. Katzung. 1985. Effects of sodium substitutes on transient inward current and tension in guinea-pig and ferret papillary muscle. *Journal of Physiology.* 360:105–120.

Bass, O. 1976. The decay of the potentiated state in sheep and calf ventricular myocardial fibers: influence of agents acting on transmembrane Ca^{2+} flux. *Circulation Research.* 39:396–399.

Beeler, G. W., and H. Reuter. 1970. The relation between membrane potential, membrane currents and activation of contraction in ventricular myocardial fibres. *Journal of Physiology.* 207:211–229.

Bers, D. 1983. Early transient depletion of extracellular Ca during individual cardiac muscle contractions. *American Journal of Physiology.* 244:H462–H468.

Blaustein, M. P., and M. T. Nelson. 1982. Sodium-calcium exchange: its role in the regulation of cell calcium. *In* Membrane Transport of Cell Calcium. E. Carafoli, editor. Academic Press, Inc., London. 217–236.

Boder, G. B., R. J. Harley, and I. S. Johnson. 1971. Recording system for monitoring automaticity of heart cells in culture. *Nature.* 231:531–532.

Brady, A. J., S. Tan, and N. V. Ricchiuti. 1979. Contractile force measured in unskinned isolated adult rat heart fibres. *Nature.* 282:728–729.

Brown, A. M., K. S. Lee, and T. J. Powell. 1981. Voltage clamp and internal perfusion of single rat heart muscle cells. *Journal of Physiology.* 318:455–477.

Bucher, O. M. 1957. A photoelectric recording set for pulsation curves of heart muscle cultures *in vitro. Experimental Cell Research.* 13:109–115.

Caputo, C., F. Bezanilla, and P. Horowicz. 1984. Depolarization-contraction coupling in short frog muscle fibers. *Journal of General Physiology.* 84:133–154.

Caroni, P., and E. Carafoli. 1980. An ATP-dependent Ca^{2+} pumping system in dog heart sarcolemma. *Nature.* 283:765–767.

Chapman, R. A. 1983. Control of cardiac contractility at the cellular level. *American Journal of Physiology.* 245:H535–H552.

Cleeman, L., G. Pizarro, and M. Morad. 1984. Optical measurements of extracellular calcium depletion during a single heartbeat. *Science.* 226:174–176.

Clusin, W. T. 1981. The mechanical activity of chick embryonic myocardial cell aggregates. *Journal of Physiology.* 320:149–174.

Cohen, C. J., H. A. Fozzard, and S.-S. Sheu. 1982. Increase in intracellular sodium ion activity during stimulation in mammalian cardiac muscle. *Circulation Research.* 50:651–662.

Costantin, L. L. 1975. Contractile activation in skeletal muscle. *Progress in Biophysical and Molecular Biology.* 29:197–224.

Eisner, D. A., W. J. Lederer, and R. D. Vaughan-Jones. 1983. The control of tonic tension by membrane potential and intracellular sodium activity in the sheep cardiac Purkinje fibre. *Journal of Physiology.* 335:723–743.

Endo, M. 1977. Calcium release from the sarcoplasmic reticulum. *Physiological Review.* 57:71–108.

Fabiato, A. 1981. Myoplasmic free calcium concentration reached during the twitch of an intact isolated cardiac cell and during calcium-induced release of calcium from the sarcoplasmic reticulum of a skinned cardiac cell from the adult or rabbit ventricle. *Journal of General Physiology.* 78:457–497.

Fabiato, A. 1983. Calcium-induced release of calcium from the cardiac sarcoplasmic reticulum. *American Journal of Physiology.* 245:C1–C14.

Fabiato, A. 1985*a*. Rapid ionic modifications during the aequorin-detected calcium transient in a skinned canine cardiac Purkinje cell. *Journal of General Physiology.* 85:189–246.

Fabiato, A. 1985*b*. Simulated calcium current can both cause calcium loading in and trigger calcium release from the sarcoplasmic reticulum of a skinned canine cardiac Purkinje cell. *Journal of General Physiology.* 85:291–320.

Fabiato, A., and F. Fabiato. 1972. Excitation-contraction coupling of isolated cardiac fibers with disrupted or closed sarcolemmas. Calcium-dependent cyclic and tonic contractions. *Circulation Research.* 31:293–307.

Fabiato, A., and F. Fabiato. 1975. Contractions induced by a calcium-triggered release of calcium from the sarcoplasmic reticulum of single skinned cardiac cells. *Journal of Physiology.* 249:469–495.

Fabiato, A., and F. Fabiato. 1979. Calculator programs for computing the composition of solutions containing multiple metals and ligands used for experiments in skinned muscle cells. *Journal de Physiologie.* 75:463–505.

Fozzard, H. A. 1977. Heart: excitation-contraction coupling. *Annual Review of Physiology.* 39:201–220.

Fozzard, H. A., and G. W. Beeler. 1975. The voltage clamp and cardiac electrophysiology. *Circulation Research.* 37:403–413.

Fozzard, H. A., and D. C. Hellam. 1968. Relationship between membrane voltage and tension in voltage-clamped cardiac Purkinje fibres. *Nature.* 218:688–689.

Gibbons, W. R., and H. A. Fozzard. 1975. Slow inward current and contraction of sheep cardiac Purkinje fibers. *Journal of General Physiology.* 65:367–384.

Hamill, O. P., A. Marty, E. Neher, B. Sakmann, and F. J. Sigworth. 1981. Improved patch-clamp techniques for high resolution current recording from cells and cell-free membrane patches. *Pflügers Archiv.* 391:85–100.

Haworth, R. A., D. R. Hunter, and H. A. Berkoff. 1980. The isolation of Ca^{2+} resistant myocytes from the adult rat. *Journal of Molecular and Cellular Cardiology.* 12:715–723.

Horackova, M., and G. Vassort. 1976. Calcium conductance in relation to contractility in frog myocardium. *Journal of Physiology.* 259:597–616.

Iijima, T., H. Irisawa, and M. Kameyama. 1985. Membrane currents and their modification by acetylcholine in isolated single atrial cells of the guinea-pig. *Journal of Physiology.* 359:485–501.

Irisawa, H., and S. Kokubun. 1983. Modulation by intracellular ATP and cyclic AMP of the slow inward current in isolated single ventricular cells of the guinea pig. *Journal of Physiology.* 338:321–337.

Isenberg, G. 1982. Ca entry and contraction as studied in isolated bovine ventricular myocytes. *Zeitschrift für Naturforschung Teil C.* 37:502–512.

Isenberg, G., A. Beresewicz, D. Mascher, and F. Valenzuela. 1985. The two components in the shortening of unloaded ventricular myocytes: their voltage dependence. *Basic Research in Cardiology.* 80(Suppl. 1):117–122.

Isenberg, G., and U. Klockner. 1982. Calcium currents of isolated bovine ventricular myocytes are fast and of large amplitude. *Pflügers Archiv.* 395:30–41.

Josephson, I. R., J. Sanchez-Chapula, and A. M. Brown. 1984*a*. A comparison of calcium currents in rat and guinea pig single ventricular cells. *Circulation Research.* 54:144–156.

Josephson, I. R., J. Sanchez-Chapula, and A. M. Brown. 1984*b*. Early outward current in rat single ventricular cells. *Circulation Research.* 54:157–162.

Keung, E. H., and R. S. Aronson. 1981. Electrophysiological properties and electrotonic interactions in hypertrophied rat myocardium. *Circulation Research.* 49:150–158.

Krueger, J. W., D. Forletti, and B. A. Wittenberg. 1980. Uniform sarcomere shortening behavior in isolated cardiac muscle cells. *Journal of General Physiology.* 76:587–607.

Kurachi, Y. 1985. Voltage-dependent activation of the inward-rectifier potassium channel in the ventricular cell membrane of guinea-pig heart. *Journal of Physiology.* 366:365–385.

Lee, K. S., and R. W. Tsien. 1982. Reversal of current through calcium channels in dialysed single heart cells. *Nature.* 297:498–501.

Lee, K. S., and R. W. Tsien. 1984. High selectivity of calcium channels in single dialysed heart cells of the guinea pig. *Journal of Physiology.* 354:253–272.

Leoty, C. 1974. Membrane currents and activation of contraction in rat ventricular fibres. *Journal of Physiology.* 239:237–249.

Leoty, C., and G. Raymond. 1972. Mechanical activity and ionic currents in frog atrial trabeculae. *Pflügers Archiv.* 334:114–128.

London, B., and J. W. Krueger. 1985. The influence of inward current and depolarization on contraction in internally perfused cardiac muscle cells. *Biophysical Journal.* 47:378*a*. (Abstr.)

Marban, E., and W. G. Wier. 1985. Ryanodine as a tool to determine the contributions of calcium entry and calcium release to the calcium transient and contraction of cardiac Purkinje fibers. *Circulation Research.* 56:133–138.

Matsuda, H., and A. Noma. 1984. Isolation of calcium current and its sensitivity to monovalent cations in dialysed ventricular cells of guinea-pig. *Journal of Physiology.* 357:553–573.

Maughan, D. W., E. S. Low, and N. R. Alpert. 1978. Isometric force development, isotonic shortening, and elasticity measurements from Ca^{2+}-activated ventricular muscle of the guinea pig. *Journal of General Physiology.* 71:431–451.

McDonald, T. F., D. Pelzer, and W. Trautwein. 1981. Does the calcium current modulate the contraction of the accompanying beat? A study of e-c coupling in mammalian ventricular muscle using cobalt ions. *Circulation Research.* 49:576–583.

Mitchell, M. R., T. Powell, D. A. Terrar, and V. W. Twist. 1984. Membrane potential and

contraction in voltage-clamped cells from rat and guinea pig ventricular muscle. *Journal of Physiology.* 346:77P. (Abstr.)

Mitchell, M. R., T. Powell, D. A. Terrar, and V. W. Twist. 1985. Influence of a change in stimulation rate on action potentials, currents and contractions in rat ventricular cells. *Journal of Physiology.* 364:113–130.

Mitra, R., and M. Morad. 1985. A uniform enzymatic method for dissociation of myocytes from hearts and stomachs of vertebrates. *American Journal of Physiology.* 249:H1056–H1060.

Morad, M., and Y. Goldman. 1973. Excitation-contraction coupling in heart muscle: membrane control of development of tension. *Progress in Biophysics and Molecular Biology.* 27:257–313.

New, W., and W. Trautwein. 1972. The ionic nature of slow inward current and its relation to contraction. *Pflügers Archiv.* 334:24–38.

Noble, D. 1984. The surprising heart: a review of recent progress in cardiac electrophysiology. *Journal of Physiology.* 353:1–50.

Ochi, R., and W. Trautwein. 1971. The dependence of cardiac contraction on depolarization and slow inward current. *Pflügers Archiv.* 323:187–203.

Reuter, H., and H. Sholz. 1977*a*. A study of the ion selectivity and the kinetic properties of the calcium dependent slow inward current in mammalian cardiac muscle. *Journal of Physiology.* 264:17–47.

Reuter, H., and H. Sholz. 1977*b*. The regulation of the calcium conductance of cardiac muscle by adrenaline. *Journal of Physiology.* 264:49–62.

Roos, K. P., A. J. Brady, and S. T. Tan. 1982. Direct measurement of sarcomere length from isolated cardiac cells. *American Journal of Physiology.* 242:H68–H78.

Schneider, M. F. 1981. Membrane charge movement and depolarization-contraction coupling. *Annual Review of Physiology.* 43:507–517.

Sheu, S.-S., and H. A. Fozzard. 1982. Transmembrane Na^+ and Ca^{2+} electrochemical gradients in cardiac muscle and their relationship to force development. *Journal of General Physiology.* 80:325–351.

Sulakhe, R. V., and P. J. St. Louis. 1980. Passive and active calcium fluxes across plasma membranes. *Progress in Biophysics and Molecular Biology.* 35:135–195.

Trautwein, W., T. F. McDonald, and O. Tripathi. 1975. Calcium conductance and tension in mammalian ventricular muscle. *Pflügers Archiv.* 354:55–74.

Wier, G. 1980. Calcium transients during excitation-contraction coupling in mammalian heart: aequorin signals of canine Purkinje fibers. *Science.* 207:1085–1087.

Wood, E. H., R. L. Heppner, and S. Wiedmann. 1969. Inotropic effects of electric currents. I. Positive and negative effects of constant electric currents or current pulses applied during cardiac action potentials. II. Hypotheses: calcium movements, excitation-contraction coupling and inotrophic effects. *Circulation Research.* 24:409–445.